Supplemental Methods (Wittmann et al.)

Quantitative analysis of nuclear infoldings in brain sections

The brains of perfusion-fixed rats were cut with a HM 650V vibratome (Microm, Walldorf, Germany). Sections containing the hippocampus were subsequently embedded as described below in 'Transmission Electron microscopy'. The resin blocks were trimmed in the shape of a cut pyramid and a semithin section was cut for orientation where the area of interest (i.e., the CA1 region) was located. The resin block was trimmed smaller so that it predominantly contained the CA1 pyramidal layer, where most nuclei belong to pyramidal neurons. Finally, serial 1.5 µm semithin sections were cut with a histo-jumbo diamond knife (Diatome AG, Biel, Switzerland) as described in Blumer et al. (2002). Glue (diluted Pattex compact, Henkel, Düsseldorf, Germany) was applied to the leading face of the pyramid, which helped the semithin sections to form ribbons. These ribbons were removed from the knife-edge using an eyelash and the ribbons were mounted onto coverslips, which were made hydrophilic by storage in water for at least 16 hours. The sections were stretched on a hot plate and stained. To determine the fraction of cells with nuclear infoldings, light microscopy images of consecutive semithin sections were taken. Nuclei were scored as 'infolded' if inspection of the serial, consecutive sections revealed the presence of at least one large membrane invagination that spans at least one third of the maximum distance across the nucleus. A total of 676 nuclei in the CA1 pyramidal layer of

P5 rats and of 947 nuclei of adult rats were analyzed. One example of a semithin section from the CA1 pyramidal layer of a P5 rat containing a highly infolded nucleus is shown in **Supplemental Figure 1**.

Transmission Electron Microscopy

For electron microscopy, cultured hippocampal neurons were fixed with 2% glutaraldehyde in 0.1 M sodium cacodylate, pH 7.4. Rat brain tissue was prepared as follows. The rats were deeply anesthetized and perfused transcardially with 2% glutaraldehyde/2% polyvidone 25/0.05% $CaCl_2$ in 0.1 M sodium cacodylate. Brains were removed from the skull and fixed further. Sections (200 µm) were cut with a HM 650V vibratome (Microm, Walldorf, Germany). All samples were washed with 0.1 M sodium cacodylate, post-fixed with 1% OsO_4/1.5% $K_4[Fe(CN)_6]$, contrasted en bloc with uranyl acetate, dehydrated with a graded series of ethanol, and embedded into glycid ether 100-based resin. Ultrathin sections were cut with a Reichert Ultracut S ultramicrotome (Leica Microsystems, Wetzlar, Germany). They were contrasted with uranyl acetate and lead citrate (Reynolds, 1963) and examined in an electron microscope (EM 10 CR; Carl Zeiss NTS, Oberkochen, Germany) at an acceleration voltage of 80 kV.

Algorithm for 3D image reconstruction

Three-dimensional (3D) image reconstruction of cell nuclei combines advanced image filtering methods with surface identification to produce a closed surface

triangulation for simulation purposes. It was done in two steps. First, the raw data sets obtained with the confocal laser scanning microscope were enhanced by applying an improved version of the nonlinear anisotropic filter described previously (Broser et al., 2004). Unlike common nonlinear, anisotropic diffusion filters, the inertia-based filter optimally enhances two-dimensional substructures in a three-dimensional domain, smoothes the nuclear membrane, closes gaps in the membrane-recording, enhances the signal to noise ratio but leaves membrane thickness unaffected. To identify two-dimensional substructures, structure-detection using the physical moments of inertia was implemented in the anisotropic filter algorithm. Having enhanced the signal to noise ratio, noise was separated from the signal, using the segmentation method of Otsu (Otsu, 1979). Following renewed application of the inertia-based filter, the geometry of the nuclear membrane was extracted. In the second step, the membrane surface was captured as a triangular surface grid which functions as the geometry model for our mathematical simulations. The triangular grid had been calculated using a marching tetrahedral method and then visualized using *VTK* (Schroeder et al., 2002). To determine the surface and volume of cell nuclei, a tetrahedral volume grid was generated with *ICEM CFD* (http://www.ansys.com/products/icemcfd.asp). Surface and volume were calculated from the triangular surface grid and the tetrahedral volume grid.

Inertia-based filter

The inertia-based diffusion filter makes use of the local moments of inertia to identify local structures of the raw microscopy data. Image data in a defined area is interpreted as a physical mass distribution. In respect to this distribution, the moment of inertia can be defined as

$$\mathfrak{M}_{\mathfrak{J}}(\mathfrak{x}^0) = \int^{\mathfrak{B}^{\mathfrak{d}}(\mathfrak{x}^0)} \mathfrak{u}(\mathfrak{x})(\mathfrak{x} - \mathfrak{M}_{\mathfrak{I}}(\mathfrak{x}^0)) \otimes (\mathfrak{x} - \mathfrak{M}_{\mathfrak{I}}(\mathfrak{x}^0))\mathfrak{q}\mathfrak{x}$$

with mass

$$M^0(x_0) = \int_{B_\delta(x_0)} u(x)dx$$

and the center of mass stated by

$$M^1(x_0) = \frac{1}{M^0(x_0)} \int_{B_\delta(x_0)} u(x)xdx$$

Having calculated the eigenvalues and eigenvectors of the inertial tensor, diffusion can be directed in the two main directions, i.e. the nuclear membrane, and blocked perpendicular to it (i.e. the third eigenvector direction) thus achieving data-sensitive filtering. The inertia-based filter used for 3D reconstructions proves to be superior in processing image data with the objective of keeping biological features unaffected and at the same time enhancing signal to noise ratios and enhancing the connectivity in the nuclear envelope. Further mathematical details and the comparison of this method of image processing to other state of the art image filters have been described in Queisser et al., 2008.

Grid-generation

From processed microscopy data, a surface grid can be computed by applying an isosurface-generating algorithm. With a defined grey value and an image-scanning cube divided into tetrahedra the image data is interpolated along the tetrahedral edges and locates the position of the defined grey value. All grid points determined by this method are then connected to a triangular grid, which represents the nuclear morphology in three dimensions. Further mathematical details have been described in Queisser et al., 2008.

Mathematical modeling

The simulation environment *UG* (Bastian et al., 2000) offers the necessary tools for numerical calculations of diffusion processes on highly unstructured geometries. It was used for implementing a mathematical model in three dimensions based on the real reconstructed geometries of hippocampal neuron nuclei and on experimentally measured data. In order to generate real 3D simulation geometries, we applied our reconstruction tools for nuclei to retrieve surface and volume grids as numerical representations of nuclei from raw confocal microscopy data of hippocampal neuron nuclei. As boundary conditions for the calcium diffusion equation, we designed the option to include cytosolic calcium transients (CCTs) that were recorded experimentally. The amplitude and frequency of these CCTs could be modified if necessary. We chose the diffusion coefficient for calcium from the interval of 13-65 $\mu m^2/s$ (Allbritton et al., 1992). Numerical multi-grid solvers were used to solve the

discrete diffusion equation, discretized with a finite volume method for the nuclear geometry and an implicit time discretization.

The model can be described as follows:

$$\begin{aligned} \left.\frac{\partial u}{\partial t}\right|_{\Omega} &= div(D\nabla u) \\ u|_{\partial\Omega} &= \text{Cytosolic calcium transient} \\ u|_{t=0} &= \text{Basal calcium concentration} \end{aligned}$$

where D denotes the diffusion coefficient for nuclear calcium, Ω the interior of the nucleus and $\partial\Omega$ the nuclear envelope. The nuclear envelope contains a numerical representation of the nuclear pore complexes by defining CCT-entry points on $\partial\Omega$ and Neumann zero conditions else. The diffusion coefficient for nuclear calcium is investigated in Allbritton et al., 1992. These values could be verified by an inverse mathematical model for parameter estimation of nuclear calcium driven by data from laser-assisted calcium uncaging experiments (data not shown). Therefore, a diffusion coefficient of 40 $\mu m^2/s$ for nuclear calcium was computed as a representative value. Since the pathways for cytosolic calcium transients are not fully understood, we recorded the cytosolic calcium transients experimentally and used these as the boundary conditions for our mathematical model. Our model only includes the nucleus; the cytosol is represented as the boundary conditions of the model.

We set up the mathematical discretization of the nuclear geometry by computing a tetrahedral volume grid for the interior of the nuclei and a triangulation of the

surface. In *UG*, multi-grid solving methods for the finite volume discretization are implemented and used for solving the discretized diffusion equation. Stating the weak formulation of the diffusion equation

$$\int_\Omega \frac{\partial u}{\partial t} = \int_\Omega div(D\nabla u)$$

and applying the Gaussian theorem yields

$$\frac{\partial}{\partial t}\int_\Omega u = \int_{\partial\Omega} D\nabla u\vec{n}$$

where $\vec{n}$ is the normal vector to the corresponding boundary surface $\partial\Omega$. Applying this equation to a single control volume b_i of the space discretizing grid and approximating the integrals numerically, yields the following equation:

$$|b_i|(u(t_{k+1},x_i)-u(t_k,x_i)) = \Delta t\sum_{j,l}|\partial b_i \cap \partial b_l| u(t_{k+1},x_j)D\cdot\nabla\xi_j(x_{il})\cdot\vec{n}_{il}$$

with $u(t_k,x_i)$ the solution of the diffusion equation in point x_i at time t_k, Δt the time step width, ∂b_i the boundary surface of the control volume b_i, ξ_i the Ansatzfunctions and $\vec{n}_{il}$ the normal vector to the corresponding surface. Together with the initial- and boundary conditions this discrete form of the diffusion model can be solved in our simulation environment *UG*.

Combined patch clamp and calcium imaging

Whole-cell patch clamp recordings were made from cultured hippocampal neurons plated on coverslips submerged in CO_2-independent buffered salt-

glucose-glycine (SGG) solution [containing (in mM) NaCl 140.1, KCl 5.3, $MgCl_2$ 1.0, $CaCl_2$ 2.0, HEPES 10.0, glycine 1.0, glucose 30.0, and sodium pyruvate 0.5] in a recording chamber (PM-1; Warner Instruments, Hamden, CT, USA) mounted on a fixed-stage upright microscope (BX51WI; Olympus, Hamburg, Germany). Patch electrodes (3-4 MΩ) were made from borosilicate glass (1.5 mm, WPI, Sarasota, FL, USA) and filled with a potassium methylsulphate based intracellular solution (containing in mM: KCH_3SO_4 135; NaCl 8; KCl 12; HEPES 10; K_2-phosphocreatine 10; Mg_2-ATP 4; Na_3-GTP 0.3; pH 7.35 with KOH). Recordings were made with a Multiclamp 700B amplifier, digitized through a Digidata 1322A A/D converter, acquired and analyzed using pClamp software (Axon Instruments, Union City, CA, USA). All membrane potentials have been corrected for the calculated junction potential of –11 mV (JPCalc program by Dr. Peter H. Barry). Differential interference contrast optics with infrared illumination or fluorescent light generated by a monochromator coupled to a light source with a 75 W Xenon arc lamp (Optoscan and Optosource, Cairn, Faversham, UK) were used to illuminate neurons which were imaged using a 60x LUMFI NA1.1 dipping objective (Olympus, Hamburg, Germany), a CCD camera (Photometrics Coolsnap HQ; Visitron Systems, Puchheim, Germany) and a software interface (Metafluor; Universal Imaging Systems, Downington, PA, USA). Either X-Rhod-1 (50 μM) or fura-2 (150 μM) was included in the patch pipette for calcium imaging. To visualize nuclear infoldings, cells were loaded at room temperature with membrane permeable ER-Tracker blue-white DPX (for X-

Rhod-1 recordings) or ER-Tracker-AM Red (for fura-2 recordings) (1 μM, final concentration in 0.1 % DMSO) for 40 min followed by 20 min after washout to allow complete deesterification of the dye before recording. Experiments were performed at 24 °C or 32-34 °C as stated in the results text. Temperature was regulated via continuous perfusion through an in-line heated perfusion pencil (Warner Instruments SH-27B; Hugo-Sachs Elektronik, Germany). Nuclear calcium signals were generated by evoking action potentials, which were induced by the injection of current (1 to 2.5 nA for 1 ms). Each stimulation consisted of bursts (2 to 5 action potentials at 100 Hz) repeated at specific frequencies (5 or 10 Hz) for 10 to 20 s. X-Rhod-1 images were acquired at 20 to 40 Hz; fura-2 ratiometric images were acquired at 15 to 20 Hz. Calcium levels were quantified as: $\Delta F/F = (F-F0)/F0$ where F represents the average background-subtracted emission fluorescence intensity in a region of interest (ROI) and F0 represents the baseline F measured prior to each stimulation. For fura-2, calcium signals were quantified as: R = F340/F380, where R represents the ratio of background subtracted emission fluorescence intensity (F) following excitation at 340 nm and 380 nm. Comparisons of calcium signals in nuclear compartments were made from small ROIs of equal size (0.8 to 1.5 μm^2) positioned in the centre of each compartment. In both X-Rhod-1 and fura-2 experiments, images of the ER Tracker labeling were made immediately prior to and immediately following the burst protocols. Experiments in which changes had occurred in the nuclear shape or focal plane were rejected. The power peak was measured from

smoothed power density curves as the difference between the maximum power within 1 Hz of the stimulation frequency and the average power 1 to 2 Hz away on both sides of the peak.

Multi-cellular calcium imaging

For simultaneous multi-cellular calcium imaging the same equipment was used as for patch clamp experiments except that an XLUMPFL 20x objective was used. Cells were loaded for 40 min at RT with 0.4 µM X-Rhod-1-AM. For quantitative comparisons of data recorded with X-Rhod-1, calcium responses were normalized to a saturating calcium signal (F_{max}) measured in response to 50 µM ionomycin.

Calcium imaging in organotypic slice cultures

All calcium imaging in organotypic slice cultures was done on DIV 13-14 at room temperature. One day before the experiment, slices were transferred to serum-free medium (consisting of: 97.5 % Neurobasal-A (Invitrogen, Karlsruhe, Germany), 2% B27 (Invitrogen, Karlsruhe, Germany) and 1 mM L-glutamine (Sigma, Taufkirchen, Germany)) to facilitate loading of the calcium indicator Oregon green 488-AM (Invitrogen, Karlsruhe, Germany). On the day of the experiment loading solution was prepared and applied to the slices exactly following the procedure described by Takahashi et al. (2007). For imaging experiments slices were transferred to a custom-built perfusion chamber and constantly perfused with artificial cerebrospinal fluid (ACSF) containing (in mM)

NaCl 125, KCl 3.5, $CaCl_2$ 2.4, $MgCl_2$ 1.3, NaH_2PO_4 1.2, glucose 10, and $NaHCO_3$ 26. Images were acquired at a frequency of 2 Hz through a 20x water immersion objective (XLUMPLFL20xW, N.A. 0.95, Olympus, Hamburg, Germany) mounted on a fixed-stage upright microscope (BX51WI; Olympus, Hamburg, Germany) equipped with an EMCCD camera (iXon DV885, Andor, BFi OPTiLAS, Puchheim, Germany) connected through a software interface (Cell^M, Olympus, Hamburg, Germany) to a computer monitor. Fluorescent excitation light was generated by a 150W xenon arc lamp (MT10, Olympus, Hamburg, Germany). Oregon green 488 was excited at 470 nm (40 nm bandwidth). Calcium levels were quantified as: $\Delta F/F = (F-F_0)/F_0$ where F represents the average background-subtracted emission fluorescence intensity in a region of interest (ROI) and F_0 represents the baseline F measured prior to each stimulation.

References

Allbritton NL, Meyer T, Stryer L (1992) Range of messenger action of calcium ion and inositol 1,4,5-trisphosphate. Science 258: 1812-1815.

Bastian P, Johannsen K, Lang S, Nägele S, Reichenberger V, Wieners C, Wittum G, Wrobel C (2000) Parallel solution of partial differential equations with adaptive multigrid methods on unstructured grids. In: High performance computing in science and engineering. (Jäger W, Krause E, eds): Springer Verlag.

Blumer MJ, Gahleitner P, Narzt T, Handl C, Ruthensteiner B (2002) Ribbons of semithin sections: an advanced method with a new type of diamond knife. J

Neurosci Methods 120: 11-16.

Broser PJ, Schulte R, Lang S, Roth A, Helmchen F, Waters J, Sakmann B, Wittum, G (2004) Nonlinear anisotropic diffusion filtering of three-dimensional image data from two-photon microscopy. J Biomed Opt 9: 1253-1264.

Otsu N (1979) Threshold selection method from gray-level histograms. IEEE Trans Sys Man Cyber 19: 62-66.

Queisser G, Wittmann M, Bading H, Wittum G (2008). Filtering, reconstruction and measurement of the geometry of nuclei from hippocampal neurons based on confocal microscopy data. J Biomed Opt 13: 014009.

Reynolds ES (1963). The use of lead citrate at high pH as an electron-opaque stain in electron microscopy. J Cell Biol 17: 208-212.

Schroeder W, Martin K, Lorensen B (2002) The Visualization Toolkit. An Object-Oriented Approach To 3D Graphics. 3nd ed. Kitware, Inc. ISBN 1-930934-07-6.

Takahashi N, Sasaki T, Usami A, Matsuki N, Ikegaya Y (2007) Watching neuronal circuit dynamics through functional multineuron calcium imaging (fMCI). Neurosci Res 58: 219-225.

Legends to Supplemental Figures (Wittmann et al.)

Supplemental Figure 1. A typical image of a serial semithin section (1.5 µm) of the CA1 pyramidal layer of a P5 rat that was used for the quantitative analysis of nuclear infoldings in brain sections. The section was stained with methylene blue/azure II. The arrow marks a highly infolded nucleus. Scale bar is 10 µm.

Supplemental Figure 2. Electron micrographs of ultrathin resin sections of the subcallosal zone of P5 rats. (**a**) Low magnification view illustrating many irregularly shaped nuclei (N). (**b-d**) High magnification view of lobular nuclei. Insert in (**c**) shows nuclear envelope on both sides of a chromatin sheet. N, nucleus. Scale bars are 1 µm.

Supplemental Figure 3. Fura-2 imaging of calcium signals evoked by 5 Hz AP bursting in a neuron with three unequally-sized nuclear compartments.

A, B) Ratiometric fura-2 calcium signals measured at 15 Hz in the regions of interest indicated in the nuclear compartments of the ER-Tracker Red labeled neuron shown in (**B)**. Calcium levels rise in response to 5 Hz AP bursting, which began at the point indicated by the arrow. Heterogeneous compartment size was apparent at all focal planes. Scale bar is 5 µm.

C) Calcium signals (high pass filtered at 1 Hz) expanded from the region indicated by the square in (**A**).

D) The membrane potential shows 5 Hz bursting recorded in parallel with the calcium signal over the same time period as in (**C**). Bursting was induced with current injection applied via whole cell patch clamp in 5 Hz bursts (1 burst = 2 injections at 100 Hz).

E) Power spectral density plots computed by the multitaper method (FFT size - 128, 5 data tapers) for the AP bursting–induced calcium signal in each compartment. A peak is apparent around 5 Hz in all compartments but is larger in the two smaller compartments.

Supplemental Figure 4.

Live imaging of an AP bursting-induced formation of a nuclear infolding in a cultured hippocampal neuron labeled with the membrane dye, DiD. Confocal stacks covering the entire nucleus of the DiD-stained neuron were recorded over time. The images are z-stacks projected into one plane and were acquired at the indicated times after the induction of AP bursting.

Supplemental Figure 5.

Photomicrographs of a glial cell with a near-spherical nucleus (upper panels) and a glial cell containing a nucleus with a small infolding (lower panels). Glial cells present in hippocampal cultures were identified by immunostaining with an antibody to glial fibrillary acidic protein (GFAP, left panels); the nuclear envelope was identified by immunostaining with an antibody to lamin B (middle panels). The right panels show an overlay of the GFAP and lamin B immunoreactivity. A quantitative analysis revealed that about 12% of glial cell nuclei showed infoldings. The infoldings are generally less prominent than those in neurons. We did not observe a significant change in the amount of infolded glial cell nuclei after stimulation of hippocampal cultures with bicuculline for 1 h.

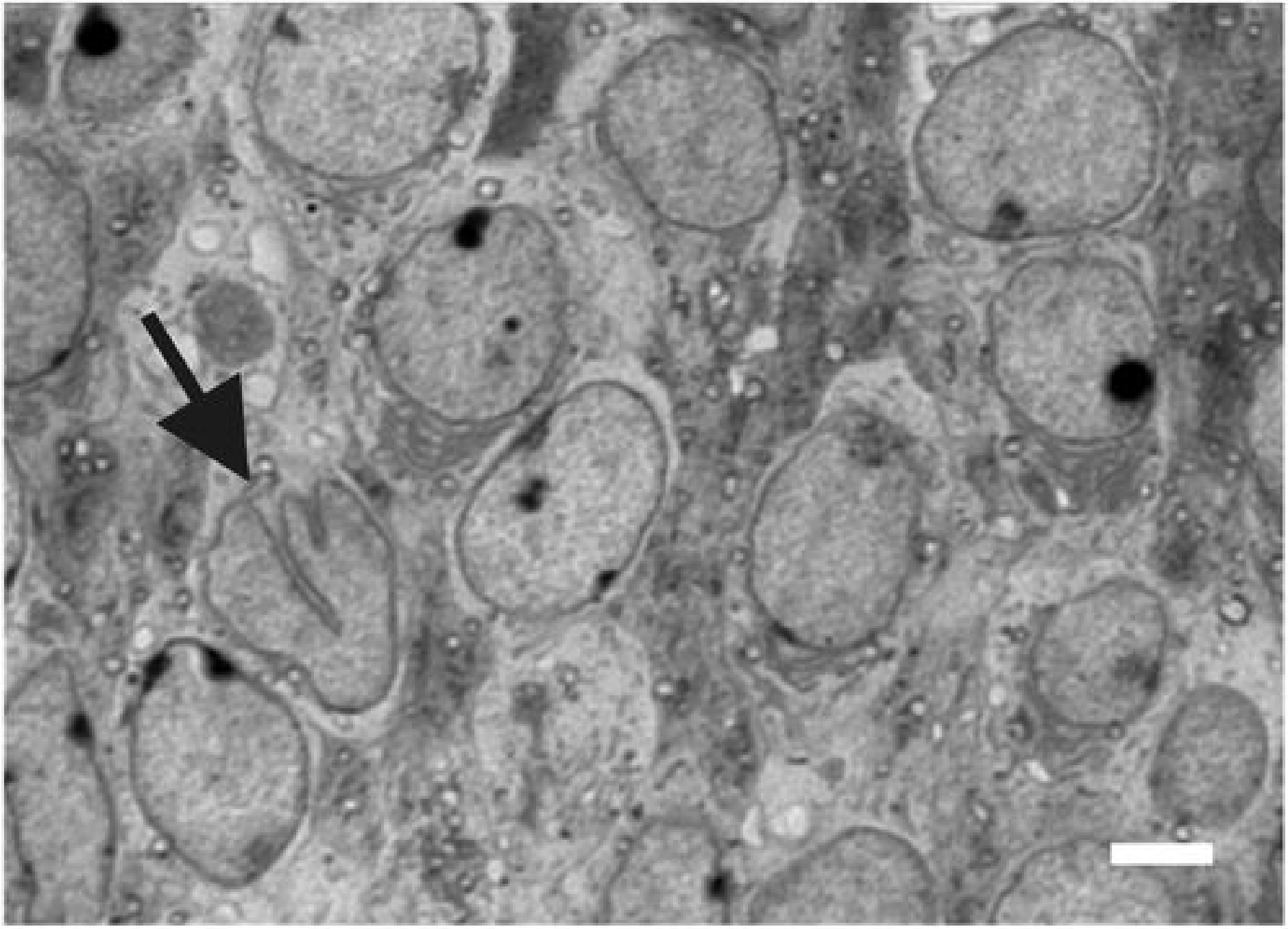

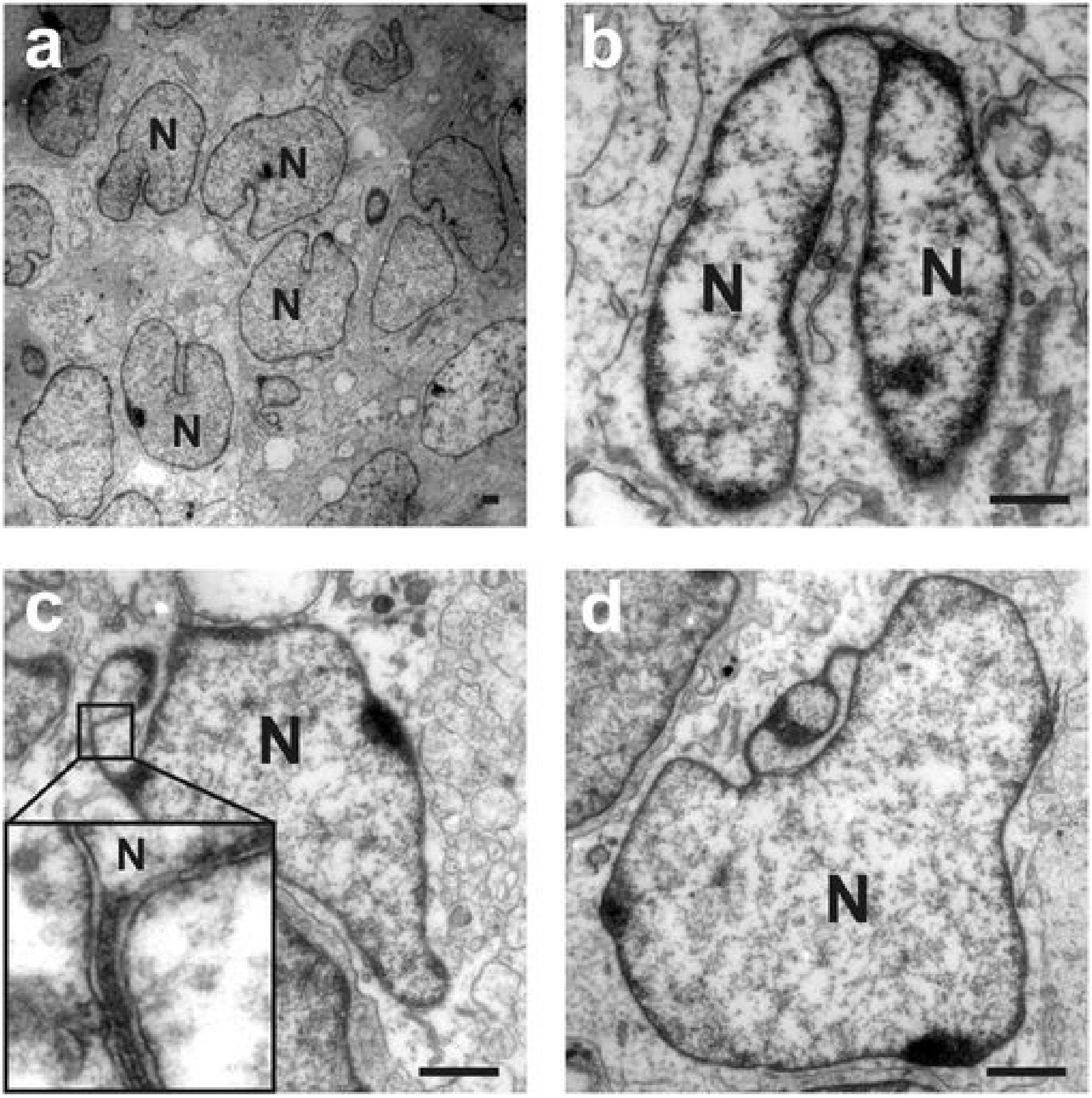
a
N
N
N
N
b
N
N
c
N
N
d
N

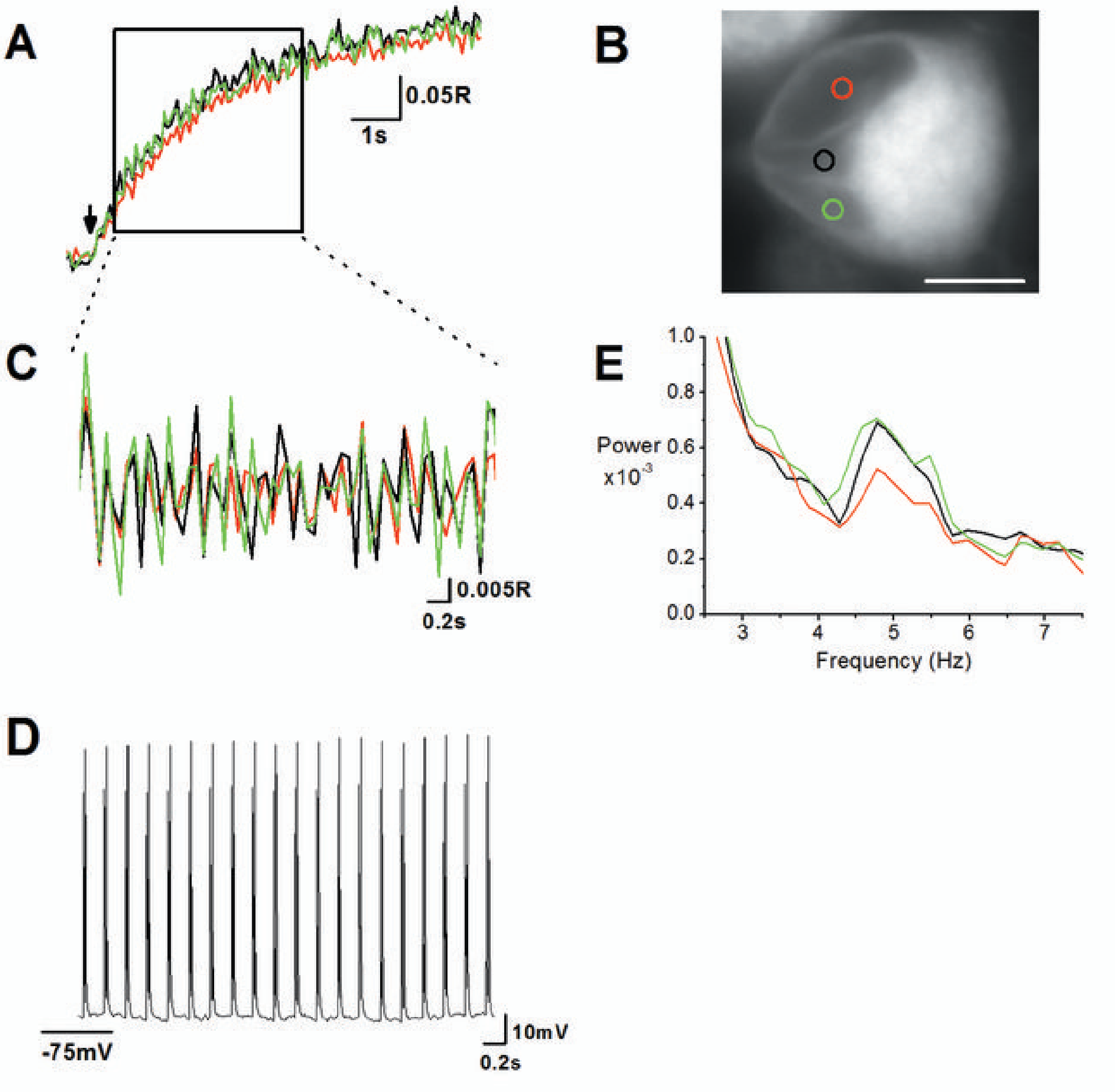
A
0.05R
1s
B
C
0.005R
0.2s
E
Power
x10-3
1.0
0.8
0.6
0.4
0.2
0.0
3
4
5
6
7
Frequency (Hz)
D
-75mV
10mV
0.2s

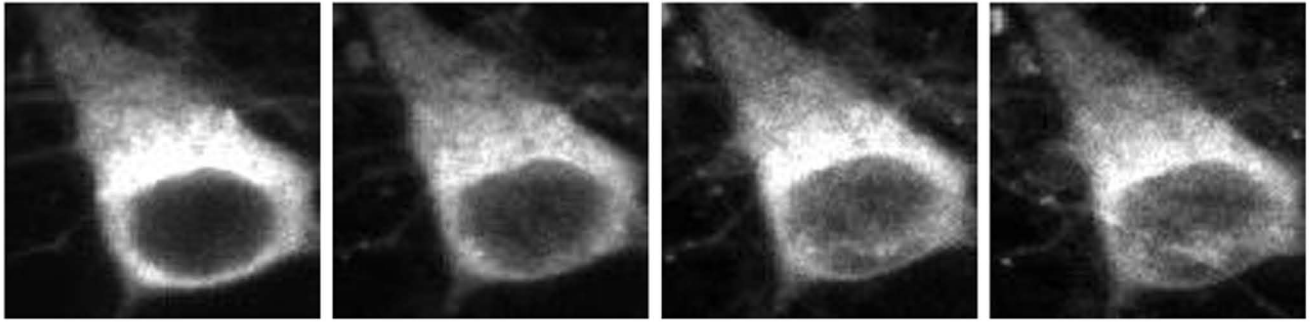
0 min
15 min
30 min
45 min

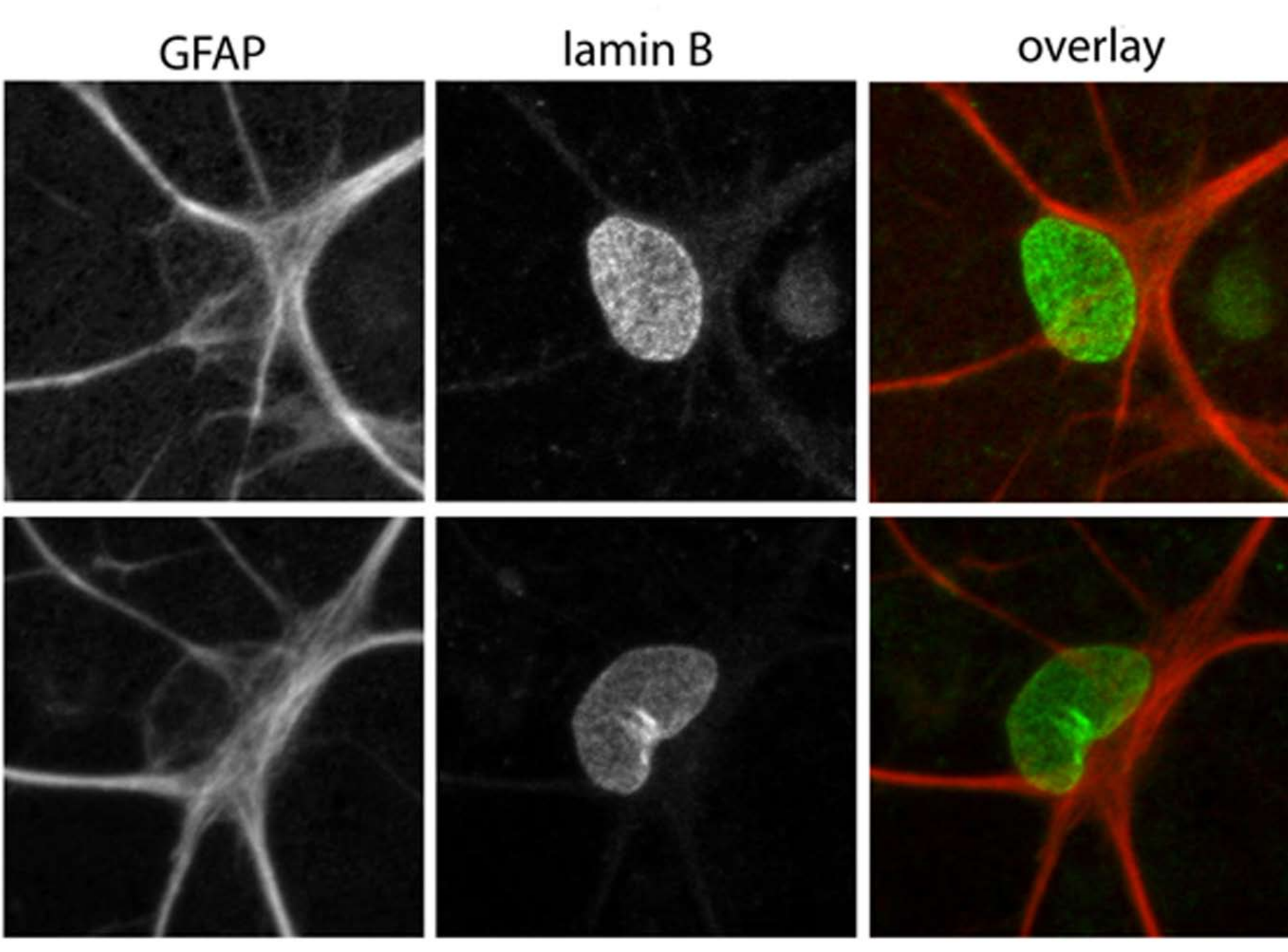
GFAP
lamin B
overlay